

# A Frequency and Polarization Reconfigurable Dual-Patch Microstrip Antenna for Wireless ISM Band

Cong Danh Bui<sup>1,2</sup>, Thanh Cuong Dang<sup>2</sup>, Minh Thuan Doan<sup>3</sup>, and Truong Khang Nguyen<sup>1,2,\*</sup>

<sup>1</sup>Division of Computational Physics, Institute of Computational Science, Ton Duc Thang University  
Ho Chi Minh City, Vietnam

<sup>2</sup>Faculty of Electrical and Electronics Engineering, Ton Duc Thang University  
Ho Chi Minh City, Vietnam

<sup>3</sup>Faculty of Electrical and Electronics Engineering, Bach Khoa University, Ho Chi Minh City, Vietnam  
\*nguyentruongkhang@tdtu.edu.vn

**Abstract** — This paper proposes a reconfigurable microstrip patch antenna design for wireless ISM band applications. The antenna simultaneously uses PIN Diodes to switch between linear and circular polarization at 2.45 GHz and uses Varactor Diode to continuously tune the operating frequency from 1.73 GHz to 2.45 GHz. The antenna performance is characterized as a combination of ON/OFF state of PIN Diode and a bias voltage of Varactor Diode varying from 0.8V to 10V. A good agreement between simulation and measurement is obtained which validates the proposed method. The proposed frequency/polarization reconfigurable antenna is promising for various applications in wireless ISM band such as DCS (1710 – 1880 MHz), PCS (1850 – 1990 MHz), GSM 1800, GSM 1900, UMTS (1920 – 2170 MHz) and WiFi/Bluetooth (2.4 – 2.5 GHz).

**Index Terms** — Frequency reconfigurable, patch antenna, polarization reconfigurable.

## I. INTRODUCTION

Reconfigurable antenna (RA) is mainly classified based on its reconfigurability which can offer single or multiple reconfiguration features such as frequency (F), bandwidth (B), polarization (P), radiation pattern (R), and a combination of them, i.e., F/B, F/R, R/P, and F/R/P [1]. Among them, F/P RAs are particularly useful in various wireless applications due to their numerous advantages such as efficient spectrum utilization, improved system capacity and flexibility, increased communication security [2]. Therefore, in the last decade, F/P RAs have attracted much attention by employing several different techniques, such as circular cavity [3], metasurface [4, 5], magnetized ferrite substrate [6], bow-tie dipole [7], liquid metal [8], etc. However, their disadvantages are complexity profile and high cost that could be unsuitable in the emergence of modern smart systems.

As a sequence, there has been increasing attention and efforts placed on designing RAs using microstrip

technology, especially microstrip patch configuration [9–17]. In [11], frequency reconfiguration was realized by switching two groups of diodes placed across the slots while another two PIN diodes were added between the input port and the 3dB hybrid coupler to achieve LHCP/RHCP reconfigurability. In [12], by using eight PIN diodes and six conductive pads, the antenna obtained the frequency reconfigurability between two WLAN bands (5.2 GHz and 5.8 GHz) and was capable of switching between linear polarization (LP) and left-hand/right-hand circular polarization (LHCP/RHCP) at each frequency. In [13], by superimposing a square ring slot into the corner truncated square patch and incorporating four PIN diodes into the square ring slot, frequency reconfigurability was obtained at two WLAN bands (5.15 - 5.35GHz and 5.75 - 5.85GHz) and polarization reconfigurability of dual-senses LP (horizontal/vertical) and CP (LHCP/RHCP) was generated at dual frequencies. In [14], by properly using a combination between PIN diodes and shorting pins, eight discrete operating frequency bands and three polarization states (LHCP/RHCP/LP) can be realized simultaneously. In [15], two switchable frequency bands were achieved by connecting an additional small patch to the main patch through a PIN diode while were also capable of operating in three polarization states (LP/LHCP/RHCP). However, the main disadvantage of these designs was that they were only able to switch between LP/CP and/or between RHCP/LHCP in a specific frequency band. Although the antenna in [9] provided a continuous and wide frequency tuning range, CP has not been reported or considered. In [10], by using 12 Varactor Diodes, frequency reconfigurability is achieved in a continuously tuned fractional bandwidth while allowing selection between CP (both rotating senses) and LP. In [16], frequency reconfigurability with continuously tunable range and polarization reconfigurability with either LP or CP (RHCP or LHCP) was achieved by using four pairs of Varactor diodes. Therefore, it can be seen that a simple

profile microstrip patch RAs that can be reconfigured in both frequency and polarization (LP and RHCP/LHCP) in a continuous frequency range is very challenging to obtain.

This paper proposes a planar microstrip dual-patch F/P RA. Two PIN Diodes work as a switch between LP and CP at 2.45 GHz while one Varactor Diode is used to tune the operating frequency from 1.73 GHz to 2.5 GHz which is able to cover many wireless applications in ISM band such as DCS (1710 – 1880 MHz), PCS (1850 – 1990 MHz), GSM 1800, GSM 1900, UMTS (1920 – 2170 MHz) and WiFi/Bluetooth (2.4–2.5 GHz). The paper will start by describing the antenna design including the bias circuit in Section 2. Then, the detailed antenna characteristics will be presented in Section 3. Finally, simulation and measurement results of the fabricated antenna at various frequencies and different polarizations will be presented and discussed in Section 4.

## II. ANTENNA AND BIAS CIRCUIT DESIGN

The antenna geometry is illustrated in Fig. 1. The radiator is comprised of primary and secondary patches that are connected together by a microstrip line. The primary patch is fed by a standard 50Ω coaxial cable and has its corners separated by PIN Diodes to create CP. The secondary patch is connected to the primary one by a transmission line that has a Varactor Diode in between functioning as a tuning element. Both patches are placed on a 1.6 mm FR-4 substrate ( $\epsilon = 4.4$ ,  $\tan \delta = 0.02$ ) with a ground plane underneath.

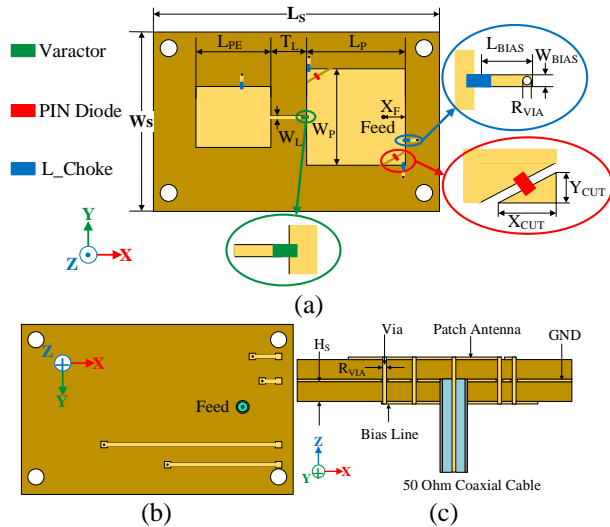


Fig. 1. Antenna geometry: (a) top view of the radiator, (b) bottom view, and (c) side view.

Another 1.6 mm FR-4 substrate is stacked underneath to support the bias circuits for PIN Diodes and Varactor Diode. A simplified bias circuit is illustrated in Fig. 2.  $V_{DC}$ ,  $R$  and *rheostat* are the components of external DC

circuits that are used to supply DC voltage for PIN Diodes and Varactor Diodes. To supply a variable voltage source, a variable resistor *rheostat* is used to change the bias voltage of Varactor Diode while a defined resistor  $R$  is used to supply a constant one for PIN Diode. A manual switch  $SW$  is also placed at PIN Diode bias line to alter the ON/OFF operating mode.  $L_{choke} = 90$  nH (LQW04CA90NK00D) is used both at each branch of active components and in front of DC source ( $V_{DC} = 12V$ ) to efficiently block RF power from the antenna.

The equivalent circuit model of PIN Diode (MADP-042305-13060) and Varactor Diode (MA46H120), found in their respective datasheets as illustrated in Fig. 3, have been used in simulation by CST Microwave Studio [18]. PIN Diode has two operating modes and each has its equivalent circuit. While mode OFF can be represented as a series circuit of  $L$  and parallel of  $R_p$  and  $C_T$ , mode ON is represented by a series circuit of  $L$  and  $R_s$ . On the other hand, Varactor Diode can be characterized by a parallel circuit of  $C_p$  and series of  $L_s$ ,  $C_j$  and  $R_s$  whereas  $C_j$  value can be varied within the component's range of  $[C_{Jmin}-C_{Jmax}] = [0.14pF - 1.1pF]$ . Their respective equivalent electric models are illustrated in Fig. 3 and optimized parameters' values for the final design are listed in Table 1.

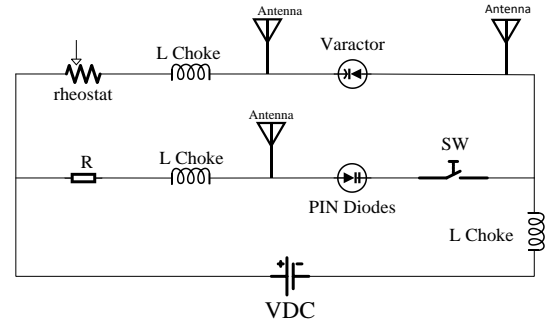


Fig. 2. Simplified bias circuit of the proposed F/P RA.

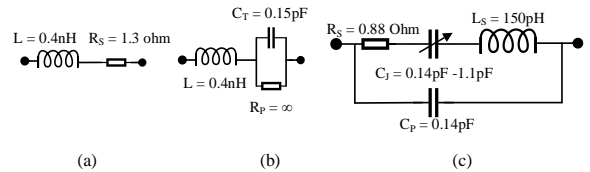


Fig. 3. Equivalent circuit of: (a) PIN Diode in ON state; (b) PIN Diode in OFF state; (c) Varactor Diode.

Table 1: Optimized values of the proposed antenna (unit: mm)

$W_s$	$L_s$	$W_p$	$L_p$	$X_f$	$T_L$	$W_L$
53	84	29	28.5	8	9.5	0.8
$L_{PE}$	$W_{PE}$	$X_{CUT}$	$Y_{CUT}$	$L_{BIAS}$	$W_{BIAS}$	$R_{VIA}$
22	18	6.4	3.7	3	0.5	0.25

### III. ANTENNA CHARACTERISTICS

#### A. Frequency reconfigurable by using varactor diode

The Varactor Diode can change the impedance and power distribution of the antenna; therefore, its resonance frequency can be shifted. Particularly, when the value of Varactor Diode reaches its greatest limit ( $C_{JMAX}$ ), the RF power transferred from the primary patch to the secondary patch is maximized. As a result, the electrical length of the antenna is then extended to its maximum possible value and has its resonance frequency the lowest. The opposite result can be concluded for the case of the minimal value of Varactor Diode ( $C_{JMIN}$ ). In short, the proposed F/P RA can have its resonance frequency highest when  $C_{JMIN}$  and lowest when  $C_{JMAX}$ . Consequently, the bandwidth tuning range can be determined within this range.

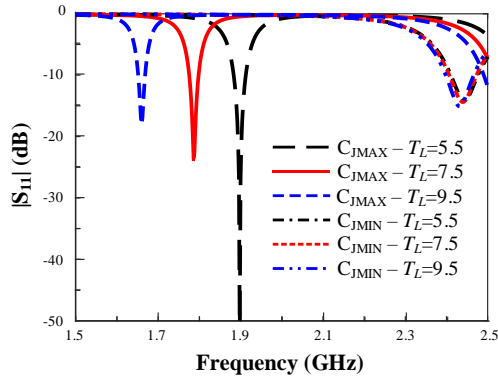


Fig. 4.  $T_L$  parameter sweep when PIN Diode is ON.

In the simulation and optimization process, it is observed that the tuning fractional bandwidth (FBW) is greatly affected by parameter  $T_L$  which is the length of the transmission line. A parameter sweep of 3 values 5.5, 7.5 and 9.5 mm when Varactor Diode's values are  $C_{JMIN}$  and  $C_{JMAX}$  was performed. As shown in Fig. 4, the lower operating frequency is shifted while the upper one remains unchanged leading to a conclusion that tuning bandwidth is affected by this transmission line length significantly. It can be seen that the resonance frequencies of the antenna at these three lengths are 1.936 GHz and 2.44 GHz, 1.786 GHz and 2.44 GHz, and 1.66 GHz and 2.43 GHz when Varactor Diode's value is  $C_{JMAX}$  and  $C_{JMIN}$ , respectively. Maximum E-field distributions at their low operating frequencies are illustrated in Fig. 5. In all 3 cases, E-field distribution is emphasized at the patch's edges in the x-direction, which is the characteristic of patch antenna [19]. Moreover, the fields are strongest at the Varactor Diode as it serves as a tunable power supply line for the secondary patch. However, the main difference can be seen in the gap between the primary and secondary patch. The edges of the two patches act as two parallel metal plates with distance  $T_L$  and form a coupling capacitor ( $C_{coupling}$ ). While performing the change

of the transmission line length,  $C_{coupling}$  has its value smallest when  $T_L = 9.5$  mm and highest when  $T_L = 5.5$  mm. This behavior has led to variation in RF power coupled between 2 patches and an abrupt difference in bandwidth tuning range. It can be found in the simulation that  $T_L$  of 9.5 mm has been chosen to have a bandwidth tuning range entirely covering DCS, PCS, UMTS and WiFi/Bluetooth applications while maintaining good gain characteristics.

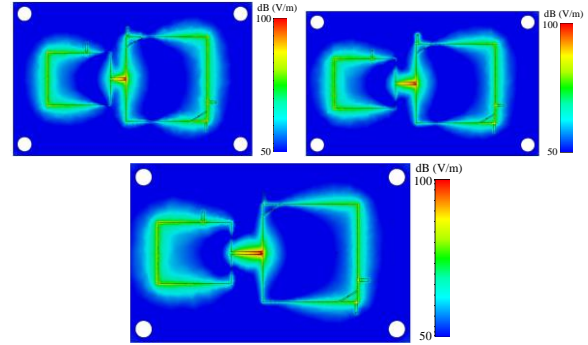


Fig. 5. Maximum E-field distribution of the proposed F/P RA: (a) at 1.918 GHz ( $T_L = 5.5$  mm); (b) at 1.778 GHz ( $T_L = 7.5$  mm); (c) at 1.66 GHz ( $T_L = 9.5$  mm).

#### B. Polarization reconfigurable by using PIN diode

As mentioned, the polarization reconfigurability of the antenna is based on the operating mode of PIN Diode. Two PIN Diodes, implemented on the gap separating the primary patch and its corners, serve as switches to create the polarization reconfigurability by connecting/disconnecting the primary patch to its corners. Since the polarization reconfigurability is created on the primary patch, Varactor Diode's value is set on  $C_{JMIN}$  to choke the RF power transferring to the secondary patch. Therefore, the switch between linear and circular polarization only occurs at the upper operating frequency, WiFi/Bluetooth application. A parameter sweep of  $X_{cut}$  from 5.5 mm to 6.1 mm and 6.7 mm, while switching PIN Diode mode ON/OFF, was performed and illustrated in Fig. 6. In Fig. 6 (a),  $|S_{11}|$  results indicate that there is little change in operating frequency between these three values when PIN Diode is OFF and ON. The Axial Ratio (AR) performance of the antenna is shown in Fig. 6 (b). It is observed clearly that polarization reconfigurability can be switched between circular and linear polarization when PIN Diode mode is OFF and ON, respectively. There is a slight change in AR resonant frequency with respect to the variation of  $X_{cut}$ . Finally,  $X_{cut} = 6.1$  mm has been chosen as the optimized value for the best AR performance.

To further verify the polarization reconfigurability of the design, the current distributions of the proposed F/P RA at 2.46 GHz when PIN Diode is OFF and ON at  $C_{JMIN}$  value of Varactor Diode are shown in Fig. 7. As shown in Fig. 7 (a) and Fig. 7 (b) with  $90^\circ$  phase

difference, not only the magnitude is similar but also the direction of the current is rotated 90° counterclockwise. Therefore, it can be concluded that the antenna exhibits right – hand CP when PIN Diode is OFF. A summary of antenna operating cases can be found in Table 2.

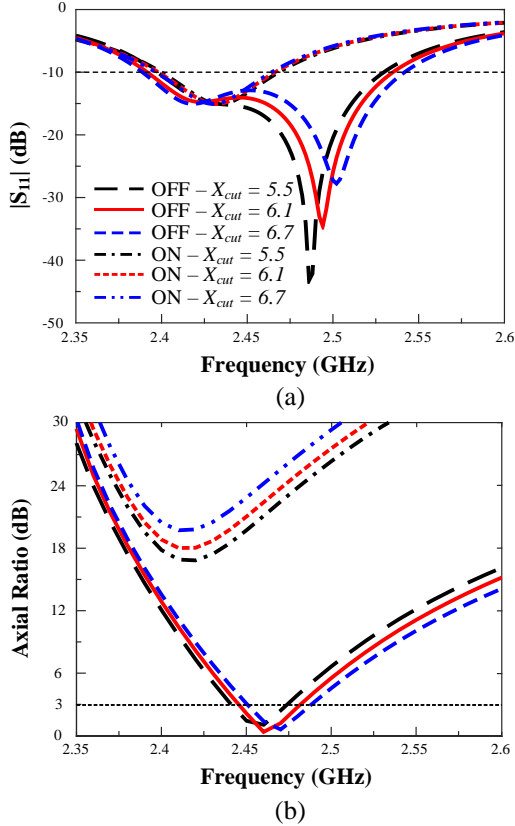


Fig. 6.  $X_{cut}$  parameter sweep while Varactor Diode's value is  $C_{JMIN}$ . (a)  $S_{11}$ ; (b) axial ratio.

Table 2: Summary of operating cases of the proposed F/P RA

Case	PIN Diode	Varactor Diode	Antenna Performance
1	OFF	$C_{JMIN}$	- 2.4 GHz – 2.5 GHz - Polarization: Circular - WiFi/Bluetooth
2	ON	$C_{JMIN}$	- 2.4 GHz – 2.5 GHz - Polarization: Linear - WiFi/Bluetooth
3	ON	$C_{JMIN} - C_{JMAX}$	- 1.73 GHz – 2.45 GHz - Polarization: Linear - DCS, PCS, GSM, UMTS, WiFi/Bluetooth

Based on the observed results, a design procedure is provided as follows:

- Design a linear polarization patch antenna at

WiFi/Bluetooth application, its initial dimension can be calculated using (1) [19]:

$$W_p = L_p \approx \frac{c_0}{2f_0\sqrt{\epsilon_r}} \tag{1}$$

Where  $c_0$  is the velocity of light in free-space,  $f_0$  is the desired operating frequency and  $\epsilon_r$  is the permittivity of the substrate.

- Detach two opposite corners from the patch by a small gap which will be used to place PIN Diode to achieve polarization reconfigurability.
- Design and connect the secondary patch to the primary one by a Transmission Line and a Varactor Diode. Note that parameter TL should be chosen carefully to acquire the desired tuning range and antenna gain characteristics.
- Add the bias circuit for both Varactor diode and PIN diode and finalize the antenna design performance.

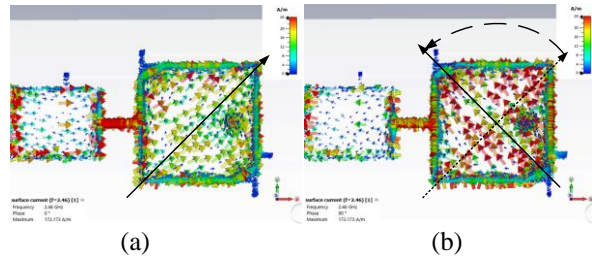


Fig. 7. E-field distribution to prove CP of the proposed F/P RA at 2.46 GHz when PIN Diode's state is OFF and Varactor Diode's value is  $C_{JMIN}$ : (a) 0° and (b) 90°.

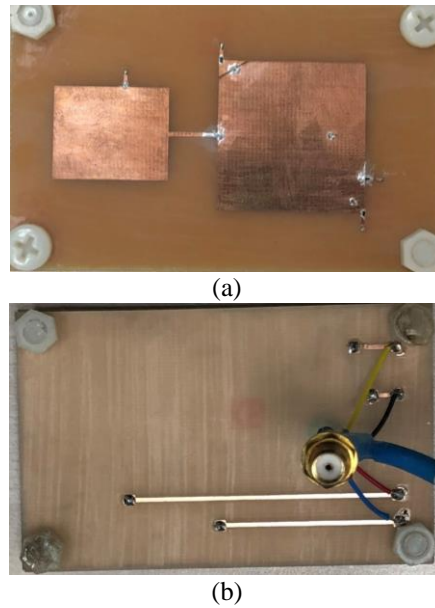


Fig. 8. Fabricated antenna design: (a) top view; (b) bottom view.

### IV. SIMULATION AND MEASUREMENT RESULTS

The proposed F/P RA is fabricated as shown in Fig. 8 and its performance in a comparison between measurement and simulation at various active component states are illustrated in Fig. 9 and Fig. 10. Generally, when the bias voltage is tuned from 10V to 0.8V, which corresponds to the change of Varactor Diode’s capacitor from  $C_{JMIN}$  (10V) to  $C_{JMAX}$  (0.8V), the frequency is tuned from upper band to lower band continuously. The highest and lowest resonant frequencies of measurement and simulation in that range are 2.4 GHz and 2.39 GHz at 10V and 1.75 GHz and 1.76 GHz at 0.8V, respectively. It can be concluded that in this voltage range, all resonant frequencies at their respective bias voltage in measurement and simulation are in good agreement. As seen in Fig. 9 (b), the antenna is found to have CP (Axial Ratio,  $AR < 3\text{dB}$ ) within the range of 2.45 – 2.486 GHz and 2.445 – 2.48 GHz in measurement and simulation, respectively, when PIN Diode state is OFF and a bias voltage of Varactor Diode is 10V. Particularly, the proposed antenna presents a small variation of measured gains (0.02 dBi – 2.56 dBi) among reconfigurable modes within the whole operating frequency band. The maximum gains of measurement and simulation are 2.56 dBi and 3.03 dBi (PIN Diode ON – 6V) whereas the minimum gains are -0.5 dBi and 0.02 dBi (PIN Diode ON – 0.8V), respectively. The simulated gains are slightly lower than the measured ones which could be contributed by the effects of active components and FR-4 substrate. A detailed comparison between simulation and measurement results in terms of resonance frequency,  $S_{11}$ , and broadside gain is summarized in Table 3.

The simulated and measured radiation patterns at multiple operating states are presented and compared in Fig. 10. It can be seen that PIN Diode states and the bias voltage of Varactor Diode do not change the patch-like radiation pattern characteristic of the proposed F/P RA. The main radiation beam of the antenna is maintained at broadside direction while almost completely suppressed in  $xy$  – plane, the plane of the antenna. The simulated and measured radiation patterns are in good agreement within the whole frequency range of interest.

Table 3: Comparison between simulation and measurement results of the proposed F/P antenna

$V_{Bias}$	Frequency (GHz)		$S_{11}$ (dB)		Gain (dBi)	
	Sim.	Mea.	Sim.	Mea.	Sim.	Mea.
10 V	2.40	2.39	-30	-15	3.0	2.05
8 V	2.37	2.36	-25	-17	2.95	2.1
6 V	2.34	2.33	-42	-19	3.03	2.56
4 V	2.22	2.22	-31	-17	2.8	2.2
2 V	1.88	1.88	-20	-11	0.9	-0.1
0.8 V	1.76	1.75	-17	-10	0.02	-0.5

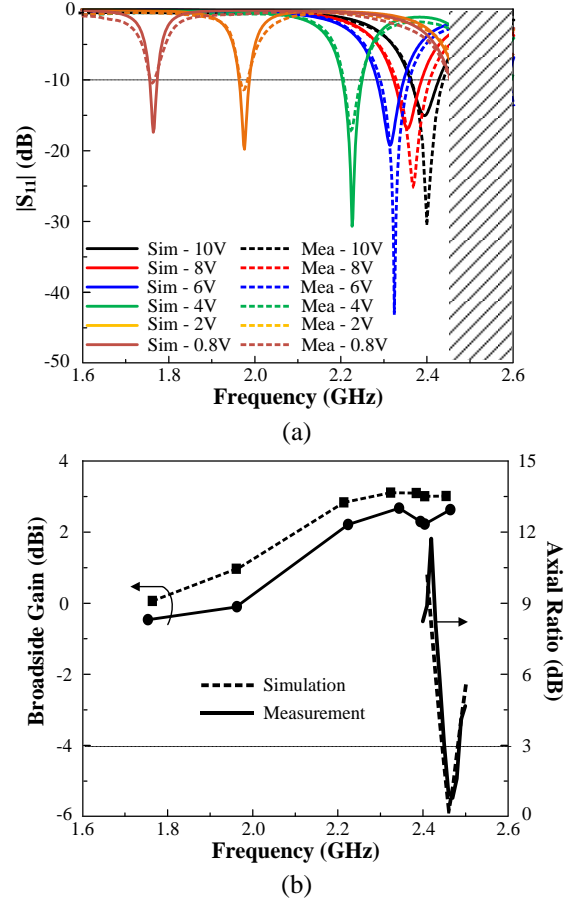


Fig. 9. Simulation and measurement results. (a) S-parameter (PIN Diode ON); (b) Gain (PIN Diode ON) and AR for CP at 2.45 GHz (PIN Diode OFF).

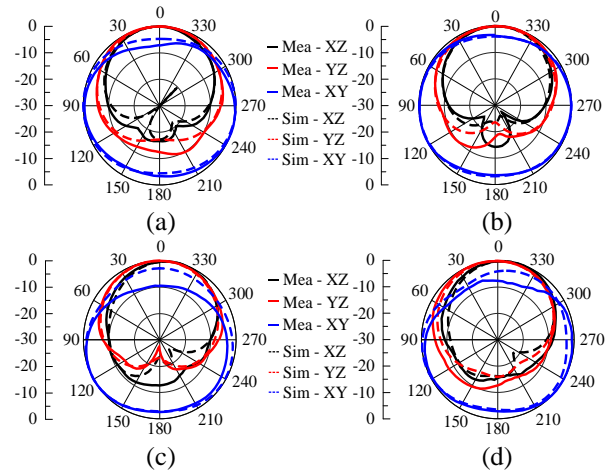


Fig. 10. Radiation patterns of the proposed F/P RA. (a) ON - 0.8 V; Mea. at 1.75 GHz, Sim. at 1.76 GHz; (b) ON - 4 V; Mea. at 2.21 GHz, Sim. at 2.22 GHz; (c) ON - 10 V; Mea. at 2.40 GHz, Sim. at 2.39 GHz; (d) OFF - 10 V; Mea. at 2.46 GHz, Sim. at 2.45 GHz.

Table 4 presents a comparative summary of the proposed RA antenna with other RAs having frequency and polarization reconfigurability. Though having dual-polarization, reconfigurable antennas in [12] and [14] using PIN Diode has a disadvantage of discrete frequency selection. On the contrary, despite having a wider band and continuous frequency tuning by using Varactor Diode, [9] and [10] only have either linear or circular polarization. The proposed antenna has shown to have both linear and circular polarization and also continuous frequency tuning within decent bandwidth while still having a simple profile.

Table 4. Comparison of proposed F/P RA with other frequency and polarization reconfigurable antenna ( $\lambda_0$  is the wavelength at the lowest operating frequency)

Ref.	Active Devices	Size ( $\lambda_0^2$ )	Frequency (GHz)	Polarization
[9]	PIN & Varactor Diode	0.3 x 0.3	1.35 – 2.25 (50%)	LP-V/ LP-H/ LP-45 <sup>o</sup>
[10]	Varactor Diode	0.5 x 0.5	2.4 – 3.6 (40%)	LHCP/ RHCP
[12]	PIN Diode	0.6 x 0.3	5.2/5.8	LP/CP
[14]	PIN Diode	0.6 x 0.3	1.85/1.95/ 2.15/2.2/ 2.35/2.45/ 2.55/2.6	LHCP/ RHCP/ LP
<b>Proposed</b>	<b>PIN &amp; Varactor Diode</b>	<b>0.5 x 0.3</b>	<b>1.73 – 2.45 (~34.4%)</b>	<b>LP/CP</b>

## V. CONCLUSION

This paper has presented a F/P microstrip dual-patch RA by using both reconfiguration means of PIN and Varactor Diodes. Despite suffering from power loss on active components and having higher cost than a conventional passive antenna, the proposed antenna can produce frequency reconfigurability with a continuously tunable range of 1.73 GHz – 2.45 GHz (~34.4%) and polarization reconfigurability with either LP and CP while having a simple profile, using fewer reconfiguration means, and achieving good/stable gain characteristics. As a result, the proposed antenna is applicable for various wireless applications in the ISM band such as DCS, PCS, GSM 1800/1900, UMTS and WiFi/Bluetooth.

## ACKNOWLEDGMENT

This research is funded by National Foundation for Science and Technology Development (NAFOSTED) under Grant No. 102.04-2019.04. The first two authors contributed equally to this work.

## REFERENCE

- [1] N. Ojaroudi Parchin, H. Jahanbakhsh Basherlou, Y. I. Al-Yasir, R. A. Abd-Alhameed, A. M.

- Abdulkhaleq, and J. M. Noras, "Recent developments of reconfigurable antennas for current and future wireless communication systems," *Electronics*, vol. 8, no. 2, p. 128, 2019.
- [2] C. G. Christodoulou, Y. Tawk, S. A. Lane, and S. R. Erwin, "Reconfigurable antennas for wireless and space applications," *Proceedings of the IEEE*, vol. 100, no. 7, pp. 2250-2261, 2012.
- [3] N. Nguyen-Trong, A. Piotrowski, L. Hall, and C. Fumeaux, "A frequency-and polarization-reconfigurable circular cavity antenna," *IEEE Antennas and Wireless Propagation Letters*, vol. 16, pp. 999-1002, 2016.
- [4] C. Ni, M. S. Chen, Z. X. Zhang, and X. L. Wu, "Design of frequency-and polarization-reconfigurable antenna based on the polarization conversion metasurface," *IEEE Antennas and Wireless Propagation Letters*, vol. 17, no. 1, pp. 78-81, 2017.
- [5] G. Liu, J. Han, X. Gao, H. Liu, and L. Li, "A novel frequency reconfigurable polarization converter based on active metasurface," *Applied Computational Electromagnetics Society Journal*, vol. 34, no. 7, pp. 1058-1063, 2019.
- [6] F. A. Ghaffar, M. Vaseem, L. Roy, and A. Shamim, "Design and fabrication of a frequency and polarization reconfigurable microwave antenna on a printed partially magnetized ferrite substrate," *IEEE Transactions on Antennas and Propagation*, vol. 66, no. 9, pp. 4866-4871, 2018.
- [7] J. Liu, J.-Y. Li, R. Xu, and S.-G. Zhou, "A reconfigurable printed antenna with frequency and polarization diversity based on bow-tie dipole structure," *IEEE Transactions on Antennas and Propagation*, vol. 67, no. 12, pp. 7628-7632, 2019.
- [8] Y. Liu, Q. Wang, Y. Jia, and P. Zhu, "A frequency-and polarization reconfigurable slot antenna using liquid metal," *IEEE Transactions on Antennas and Propagation*, 2020.
- [9] P.-Y. Qin, Y. J. Guo, Y. Cai, E. Dutkiewicz, and C.-H. Liang, "A reconfigurable antenna with frequency and polarization agility," *IEEE Antennas and Wireless Propagation Letters*, vol. 10, pp. 1373-1376, 2011.
- [10] N. Nguyen-Trong, L. Hall, and C. Fumeaux, "A frequency-and polarization-reconfigurable stub-loaded microstrip patch antenna," *IEEE Transactions on Antennas and Propagation*, vol. 63, no. 11, pp. 5235-5240, 2015.
- [11] P. Zhang, S. Liu, R. Chen, and X. Huang, "A reconfigurable microstrip patch antenna with frequency and circular polarization diversities," *Chinese Journal of Electronics*, vol. 25, no. 2, pp. 379-383, 2016.
- [12] B. Anantha, L. Merugu, and P. S. Rao, "A novel single feed frequency and polarization reconfig-

- urable microstrip patch antenna,” *AEU-International Journal of Electronics and Communications*, vol. 72, pp. 8-16, 2017.
- [13] A. Bharathi, M. Lakshminarayana, and P. S. Rao, “A quad-polarization and frequency reconfigurable square ring slot loaded microstrip patch antenna for wlan applications,” *AEU-International Journal of Electronics and Communications*, vol. 78, pp. 15-23, 2017.
- [14] J. Hu and Z.-C. Hao, “Design of a frequency and polarization reconfigurable patch antenna with a stable gain,” *IEEE Access*, vol. 6, pp. 68, 169-68, 175, 2018.
- [15] R. K. Singh, A. Basu, and S. K. Koul, “A novel reconfigurable microstrip patch antenna with polarization agility in two switchable frequency bands,” *IEEE Transactions on Antennas and Propagation*, vol. 66, no. 10, pp. 5608-5613, 2018.
- [16] H. Gu, J. Wang, L. Ge, and L. Xu, “A reconfigurable patch antenna with independent frequency and polarization agility,” *Journal of Electromagnetic Waves and Applications*, vol. 33, no. 1, pp. 31-40, 2019.
- [17] R. K. Singh, A. Basu, and S. K. Koul, “Reconfigurable microstrip patch antenna with polarization switching in three switchable frequency bands,” *IEEE Access*, vol. 8, pp. 119, 376-119, 386, 2020.
- [18] CST Microwave Studio, CST GmbH, 2016. <http://www.cst.com>
- [19] C. A. Balanis, *Antenna Theory: Analysis and Design*. 4th ed., John Wiley & Sons, ch. 14, July 2016.